# Brain activity patterns under Resting State.

Fabrizio Parente[*] and Alfredo Colosimo[*]

[*]Dept. of Anatomy. Histology. Forensic Medicine and
Orthopaedics Sapienza. University of Rome

### Abstract

Up to now positive, coactivating interactions polarized the attention of people studying the time-dependent functional connectivity of brain networks: we report here about the negative, deactivating interactions observed, in the same above contest, after filtering by appropriate thresholds the intensities of BOLD signals from coupled brain regions. The final aims of our strategy remain: 1) studying the de-activating interactions in their essential role of keeping stationary any functional brain state, and 2) exploiting the opportunity of clustering different subjects from functional parameters recorded under the favorable condition offered by the Resting State.

**Keywords.** Brain Resting State, Brain Functional Networks, time-dependent fMRI .

# 1 Introduction.

Describing the emerging complexity of interconnected functional patterns in human brain requires a set of specific analytical tools. Thus, on the basis of fMRI data, different spatial levels of interactions have been ascribed to different cortical and sub-cortical brain regions at different spatial scales [1]: from the $1\ mm^2$ of grey matter of single anatomical regions to the whole-brain functional network [2]. More recently, different kinds of brain interactions have been measured, such as correlations (or *in phase* signal dependences) and anti-correlations (or *in anti-phase* signal dependences) [3] [4] [5] [6] [7]. In addition, the time variability of the functional connections has been also explored and, in such a context, observations in different cognitive states (such as attention, motor task, ecc..) showed different patterns.

The fMRI acquisitions considered here are obtained under a *resting state condition* (subjects with open eyes in the absence of any cognitive task). To study the time-dependent functional interactions, we focussed on the sliding-window and on the Co-Activation Pattern (CAP) methods. The former one [8] based on the correlation of short time-windows (2 min) in the whole time series (8 minl) showed different functional patterns in the same subject during the same acquisition epoch and showed useful to discriminate healthy from pathological mental states in schizophrenic patients [9]. The latter one stems from the idea that filtering peacks of large amplitude by arbitrary thresholds in the BOLD signals, can occur without substantial reduction of information. Moreover, Petridou et al. [10] clarified how unexpected conditions may contribute to the correlation strength and the power spectra of slow fluctuations. From these assumptions Liu and Duyn [11] proposed the Co-Activation Pattern (CAP) analysis as an alternative to the traditional use of linear correlation. The authors suggest the use of a few critical peaks (when signal intensities overcome an arbitrary threshold) to characterize stable spatial patterns.

Along these lines, we studied the relevance of discrete phenomena in appropriately thresholded time series. Since CAP takes into account the possibility of positive co-activation among cerebral areas, we decided to extend the analysis to a more general set of possibilities , including negative interaction. In addition, by a Principal Component Analysis (PCA) , we tried and identify significant events in brain functional dynamics in the aim to characterize the individual features of the complex trends emerging from the variability of the observed phenomena.

# 2 Materials and methods.

## 2.1 Data collection and processing.

We analyzed the BOLD (Blood-Oxygen-Level Dependent) functional images of 180 healthy individuals from the Beijing Zang dataset (1000 Functional Connectomes Classic collection 1) recorded at the Imaging Center for Brain Research of the Beijing Normal University , using a 3.0 T Siemens scanner.

As detailed in the Appendix, the images of each subject were corrected by the anatomical CompCorr method [12], preprocessed by a Matlab Toolbox (CONN), and divided into 90 ROI (Regions Of Interest) by an automatic anatomical la-

beling [13]: from each ROI a corresponding time series was eventually obtained.

In agreement with Power et al. [14] we used the Framewise Displacement (FD) to look for movement variability in single scans and sign as *bad scans* movements above than $0.2mm$. Then, since artifacts can change signals after $8s$, we made a mask from the preceding to the following two scans of a *bad scan* (with $TR = 2$ this means a sequence of $8s$ in total). Finally, we scrubbed off the mask from the temporal sequences of BOLD acquisitions; if the number of slices in the temporal mask was higher then 60 (120 seconds), the subject was removed from the analysis: in total we rejected 11 subjects (see also Figure 5 in the Appendix).

## 2.2 Setting of thresholds

In order to detect the significant positive as well as negative interactions occurring among brain regions, a series of thresholds were applied to the BOLD signals normalized as z-scores within the same ROI.

Thus, we transformed the BOLD signals in series of three possible cases (activation = 1, deactivation= -1, null = 0), just on the basis of the signal intensity. As a consequence, the possible interactions between cerebral regions become $3^2 = 9$, namely :

- [1;1] and [-1;-1] (co-activations and co-deactivations)

- [1;-1] and [-1;1] (mutual deactivations)

- [0;0, 1;0, 0;1, -1;0, 0;-1] (null interactions)

The whole procedure is graphically schematized in Figure 6 in the Appendix.

## 2.3 Deriving Pointwise Mutual Information (PMI).

Pointwise Mutual Information (PMI) can be used as a measure of association. More precisely, while PMI refers to a single occurrence, the mutual information (MI) refers to the average of all possible cases. Thus, the mutual informations for a combination of activation (1) events among two brain regions is given by:

$$PMIab(1;1) = ln(Pab(1;1)/[Pa(1) * Pb(1)])$$  (1)

where a and b are the two brain regions, Pab(1;1) is the joint frequency of (1) in both regions, and Pa(1), Pb(1) are the marginal frequencies of (1) in the signals pertaining to regions a and b.

Thus, if the joint probability (numerator) is the same as the product of the marginal probabilities (denominator), the 2 events are independent; If the numerator is greater than the denominator, the 2 phenomena tend to depend among each other; the opposite can occur as a consequence of noise. In our case a negative value of PMI (logarithm lower than 1, associated with noise) is set to 0 and not considered. The procedure is schematized in the Appendix ( Figure 7).

The PMIs have been calculated for each of the 9 combinations, for all the couples (90*89/2 = 4005) of brain regions and for each threshold ($\pm$ 0.25; $\pm$ 0.50; $\pm$ 0.75; $\pm$ 1). The result is a set of 4 matrices each formed by 9 columns and 4005 rows characterizing the functional connectivity of single individual.

3

## 2.4 Statistical analyses.

In the aim to pick-up significant coupled-activations in the brain functional dynamics we applied a Principal Component Analysis (PCA) to the above data-set, separately at each threshold level, to check for a potential dependence of the phenomena from the amplitudes of BOLD signals.

In a multivariate data-set PCA finds out a new set of orthogonal variables defined as linear combinations of the original ones through the so called *loadings*. Our hope is that a significant amount of variability (information) can be associated, through the loadings, to the original variables from the clustering patterns of data in a PCA space.
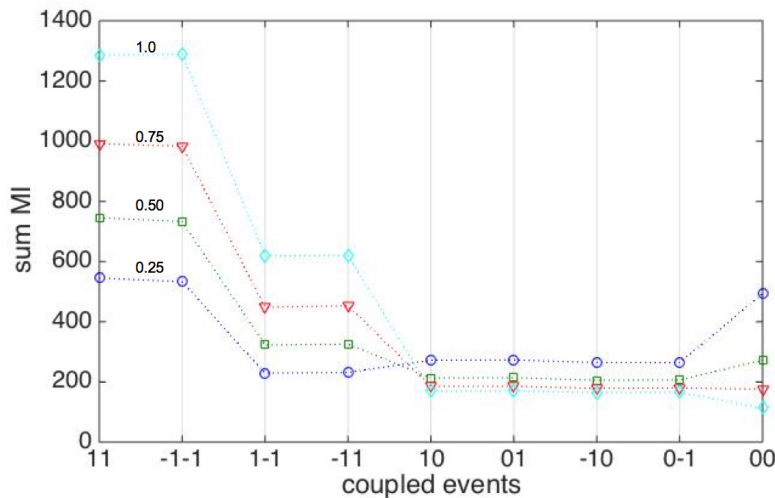


Figure 1: *Sum of the PMI of coupled activities.*
Notice that at increasing thresholds the corresponding mutual information of coupled activities [11,-1-1,1-1,-11] increases.

# 3 Results.

## 3.1 Marginal, joint frequency and PMI of thresholded neural activities.

As for the joint frequencies of the 9 differently combined activities, the values of coupled activations and deactivations decreases at increasing threshold values, while the coupled null-cases tend to increase (not shown). The corresponding PMI sums (Figure 1), however, show the opposite trend: low values at low threshold and greater values at more conservative thresholds for coupled activation and deactivation (1;1, -1;-1, 1;-1, -1;1) and the inverse trend for the coupled null cases (0;0)[1].

---

[1] The PMI sums of the remaining couples (0;1, 1;0, 0;-1, -1;0) are not sensitive to the threshold, similarly to the joint frequencies (not shown).

## 3.2 PCA analysis of PMI.

By a Principal Component Analysis (PCA) of the 4 matrices (one for each threshold), formed by 9 columns and 4005 rows characterizing the functional connectivity of each single individual, we found 4 Principal Component (PC) explaining most part of the variability. The mean values of the components for all subjects and the corresponding box plots are shown in Table 1 and in Figure 2. The similarity of such values across subjects seems to indicate

|      | PC1         | PC2         | PC3         | PC4         |
|------|-------------|-------------|-------------|-------------|
| **0.25** | 31.4 ($\pm$0.7 ) | 17.6 ($\pm$0.3) | 16.7 ($\pm$0.3 ) | 16.0 ($\pm$0.4 ) |
| **0.50** | 31.6 ($\pm$1.1) | 19.9 ($\pm$0.9 ) | 16.6 ($\pm$0.6 ) | 15.5 ( $\pm$0.6) |
| **0.75** | 32.4 ( $\pm$1.5 ) | 20.9 ($\pm$1.4 ) | 16.3 ($\pm$0.7 ) | 15.1 ( $\pm$0.7) |
| **1.0**  | 32.9 ($\pm$1.5) | 20.9 ($\pm$1.5 ) | 16.3 ($\pm$0.3) | 14.9 ($\pm$0.8) |

Table 1: *% of first 4 Principal Components at different thresholds.*
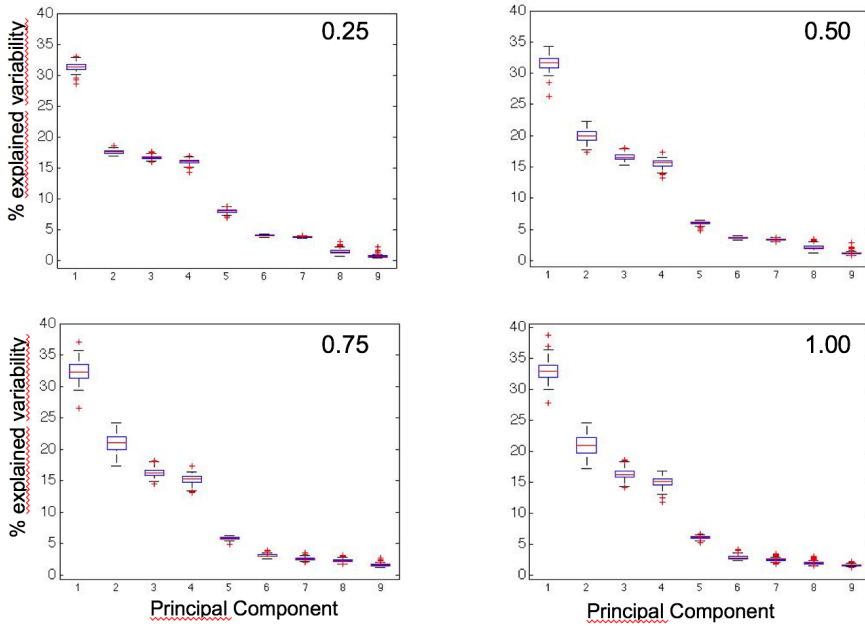


Figure 2: *Principal Components extracted from nine coupled activities (see the text).* In the upper right corner of each panel the associated threshold is reported.

their dealing with some general functional mechanism more than with subjective processes, differentiest among individuals.

As for PC1, the distribution of averaged loadings in Figure 3 (left panels) show high values for the coupled activites [1;1], [-1;-1] and [0; 0] at all the used thresholds. In the other cases the loadings become negative as the threshold increases, while the corresponding standard deviation decreases as a function of threshold values, except for [1;-1] and [-1;1] that show a small increase.

PC2, on the other hand, shows high positive loadings for the [1;-1], [-1;1] and [0;0] couples, which in the first 2 cases increase with the threshold and decrease
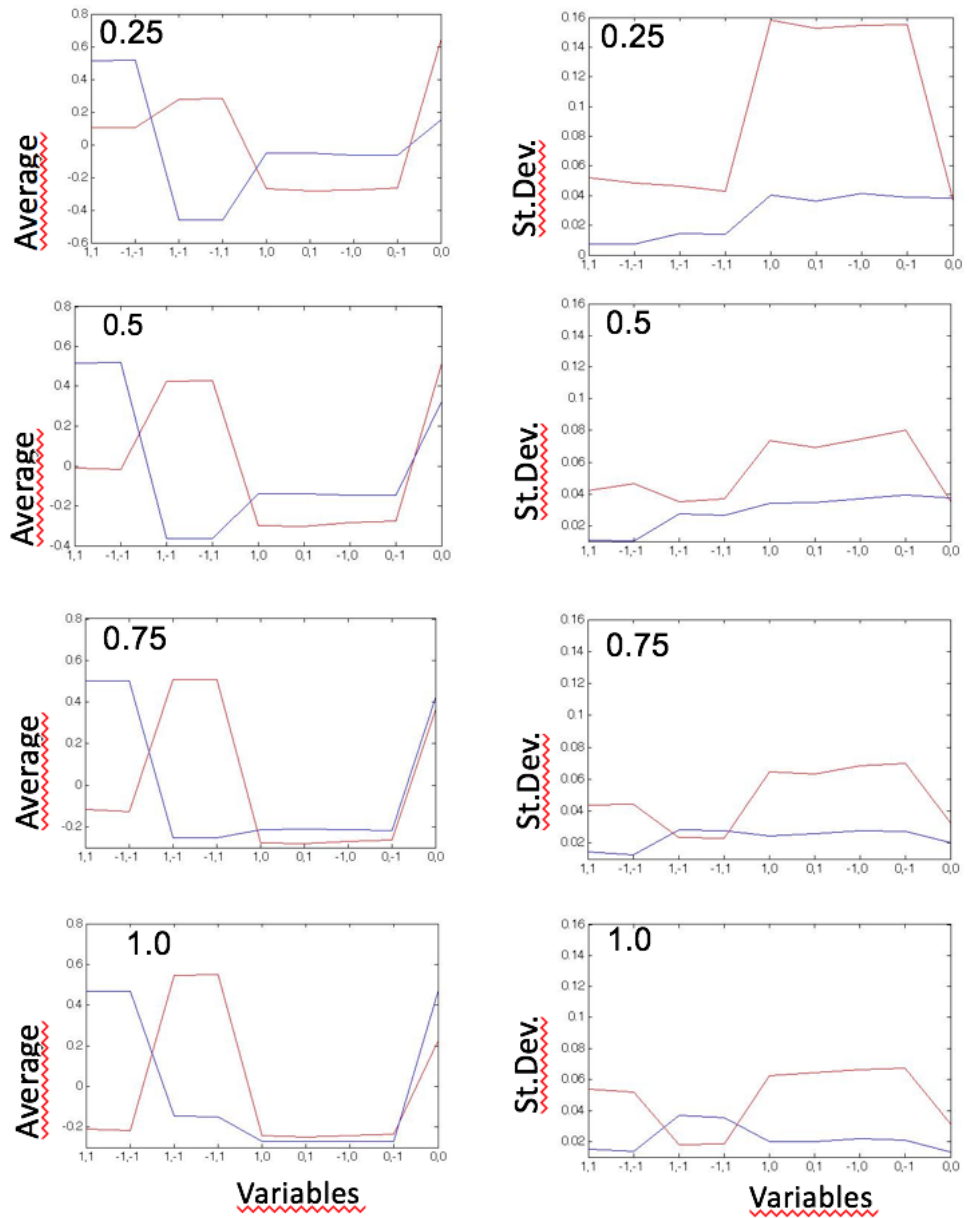
Figure 3: *Loading distribution of original variables over PC1 and PC2.*
The averaged (over individuals) loading of the original variables (coupled activities) over PC1 (blue line) and PC2 (red line) is reported in the left panels, with the corresponding St. Dev. in the right panels. In the upper left corner of all panels the associated threshold values.

in the third one. The [1;1] and [-1;-1] couples show small positive loadings in the less conservative threshold (0.25) and negative loadings everywhere else, similarly to the case of all other couples.

The loadings variability across subjects Figure 3 (right panels) decreases with thresholds mainly for [1;-1] and [-1;1]. The third and fourth PC show a more complicated behavior (not shown) in which no evident distribution pattern appears for the loading associated to each couple.

# 4    Discussion.

In this paper the activity of 90 ROI, identified in the brain BOLD functional images of 180 healthy individuals, has been followed in time for 8 minutes at a resolution of 2 seconds. Our preliminary assumption is that each single ROI may have three functional states: activated [+1], non-activated [0] and deactivated [-1] state as a result of filtering and then binarizing the intensity of time-dependent signals by appropriate thresholds. Such a procedure clearly corresponds to a noise-cleaning method in which increasing thresholds remove more and more random events from the subsequent analysis of the $3^2 = 9$ possible combinations of the three above mentioned states in coupled regions.
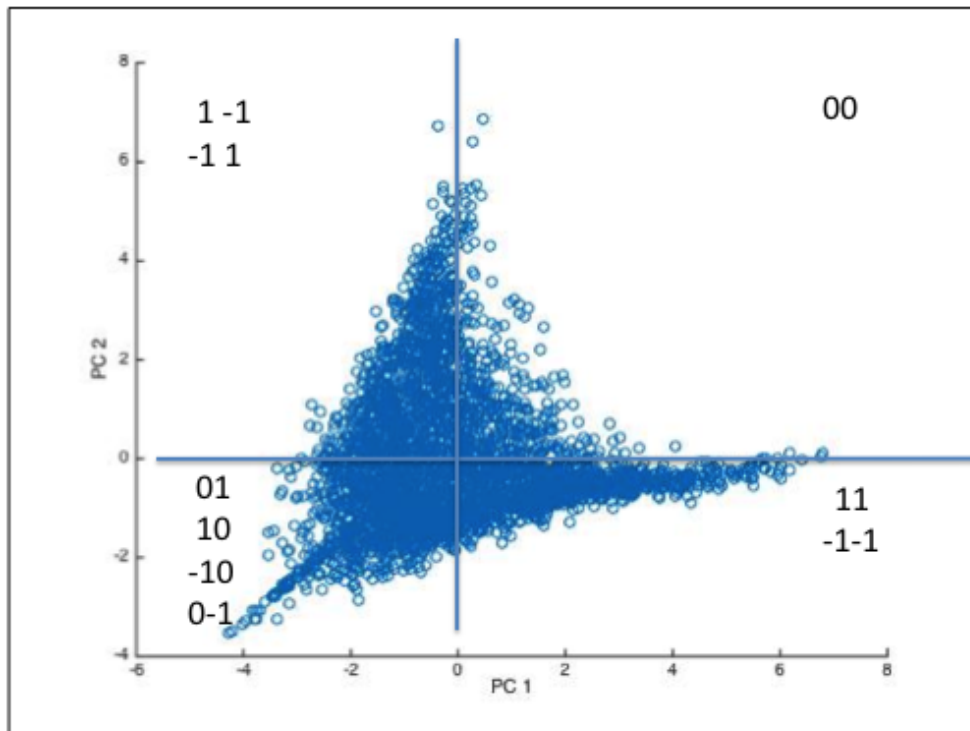


Figure 4: *Scores distribution of MI values in a PC1 / PC2 space.*
The scores are from the 90*89/2 MI values of the ROIs of a single subject reckoned from raw data filtered at the highest threshold level.

In the combined activity of paired regions, only two states of single regions

7

were considered: activated and deactivated. Thus, the possible coupled conditions become: co-activation; co-deactivation; mutual deactivation; null.

The PC1 and PC2 obtained from the multivariate analysis of such 9 possible combinations seem to indicate 2 phenomena: the first one including some co-activation [1;1] and co-deactivation [-1;-1] states, the second one related to mutual deactivation. Both phenomena are reflected by, respectively, in-phase (or positively related) and anti-phase (or negatively related) signals originated in the corresponding brain regions.

The loadings of the 9 original combination variables averaged over subjects and projected on the PC1 / PC2 space (Figure 3, left panels) reveals that the first two PCs are related to some characteristic common to most subjects[2] The same exercise carried out for each single subject should provide a reliable clustering of subjects on the basis of some unexpected simple or complex feature: at the moment this is one main goal of our investigations.

Finally, the idea that negative interactions play a basic role in the regulation mechanisms of brain functional networks, is reinforced by the plot of scores shown in (Figure 4, where co-activation [+1; +1] and co-deactivation [-1; -1] lie in the IV quadrant, while mutual deactivations, [-1; +1] and [+1; -1], in the II (and opposite) quadrant, thus pointing to independent and equally important functions.

# References

[1] Rubinov M. and Sporns O. Weight-conserving characterization of complex functional brain networks. *Neuroimage*, 56:2068–2079, 2011. 2

[2] Sporns O., Tononi G., and Kotter R. The human connectome: A structural description of the human brain. *PLoS Comput Biol.*, 1(4):e42, 2005. 2

[3] Anticevic A., Gancsos M., Murray J.D., Repovs G., Driesen N.R., Ennis D.J., Niciu M.J., Morgan P.T., Surti T.S., Bloch M.H., Ramani R., Smith M.A., Wang X.J., Krystal J.H., and P.R. Corlett. Nmda receptor function in large-scale anticorrelated neural systems with implications for cognition and schizophrenia. *Proceedings of the National Academy of Sciences of the United States of America.*, 109(41):16720–16725, 2012. 2

[4] Keller C.J., Bickel S., Honey C.J., Groppe D.M., Entz L., Craddock R.C., Lado F.A., Kelly C., Milham M., and Mehta A.D. Neurophysiological investigation of spontaneous correlated and anticorrelated fluctuations of the bold signal. *The Journal of Neuroscience*, 33(15):6333–6342, 2013. 2

[5] Keller J.B., Hedden T., Thompson T.W., Anteraper S.A., Gabrieli J.D., and Whitfield-Gabrieli S. Resting-state anticorrelations between medial and lateral prefrontal cortex: Association with working memory, aging, and individual differences. *Cortex*, 64:271–280, 2015. 2

[6] Gopinath K., Krishnamurthy V., Cabanban R., and Crosson B. A. Hubs of anticorrelation in high-resolution resting-state functional connectivity network architecture. *Brain Connectivity*, 5(5):267–275, 2015. 2

[7] Parente F., Frascarelli M., Mirigliani A., Di Fabio F., Biondi M., and Colosimo A. Negative functional brain networks. *Brain Imaging Behav.*, Mar 29:doi: 10.1007/s11682–017, 2017. 2

[8] Allen E.A., Damaraju E., Plis S.M., Erhardt E.B., Eichele T., and Calhoun VD. Tracking whole-brain connectivity dynamics in the resting state. *Cereb Cortex.*, 24(3):663–76, 2014. 2

[9] Damaraju E., Allen E.A., Belger A., Ford J.M., McEwen S., Mathalon D.H., Mueller B.A., Pearlson G.D., Potkin S.G., Preda A., Turner J.A., Vaidya J.G., van Erp T.G., and Calhouna V.D. Dynamic functional connectivity analysis reveals transient states of dysconnectivity in schizophrenia. *Neuroimage Clin.*, 5:298–308, 2014. 2

---

[2] The remaining PCs probably take into account subjective and/or random events.

[10] Petridou N., Gaudes C.C., Dryden I.L., Francis S.T., and Gowland PA. Periods of rest in fmri contain individual spontaneous events which are related to slowly fluctuating spontaneous activity. *Hum Brain Mapp.*, 34(6):1319–29, 2013. 2

[11] Liu X., Chang C., and Duyn J.H. Decomposition of spontaneous brain activity into distinct fmri co-activation patterns. *Front Syst Neurosci.*, 7:101, 2013. 2

[12] Behzadi Y., Restom K., Liau J., and Liu T. T. Acomponent based noised correction method (compcor) for bold and perfusion based fmri. *NeuroImage*, 37(1):90–101, 2007. 2, 10

[13] Tzourio-Mazoyer N., Landeau B., Papathanassiou D., Crivello F., Etard O., Delcroix N., Mazoyer B., and Joliot M. Automated anatomical labeling of activations in spm using a macroscopic anatomical parcellation of the mni mri single-subject brain. *Neuroimage*, 15(1):273–89, 2002. 3, 10

[14] Power J.D., Mitra A., Laumann T.O., Snyder A.Z., Schlaggar B.L., and Petersen S.E. Methods to detect, characterize, and remove motion artifact in resting state fmri. *Neuroimage*, 84:10, 2014. 3

# APPENDIX 1
## Data pre-processing procedures.

The 1000 Functional Connectomes Classic collection, Beijing Zang dataset, was used (`http://fcon_1000.projects.nitrc.org/indi/retro/BeijingEnhanced.html`). The database includes 180 brain functional images of healthy individuals acquired with a 3.0 T Siemens scanner and the following acquisition parameters: repetition time, 2000 ms; echo time, 30 ms; slices, 33; thickness, 3 mm; gap, 0.6 mm; field of view, 200x200 mm; resolution, 64x64; flip angle, $90^{o}$.

For the anatomical images a T1-weighted sagittal three-dimensional magnetization prepared rapid gradient echo (MPRAGE) sequence was used, covering the entire brain: 128 slices, TR= 2530ms, TE= 3.39ms, slice thickness= 1.33mm, flip angle= 7, inversion time= 1100ms, FOV= 256x256mm, and in-plane resolution= 256x192. The first 10 scans of each subject were removed, then the remaining functional images were oriented to the twentieth scan, re-aligned and co-registered to the T1 image. Both the functional and the anatomical images were normalized to standard space (EPI image in Montreal Neurological Institute coordinates) using the normalization parameters of the T1 image. Afterwards, a spatial gaussian filter was used (4x4x4mm), the motion parameters were regressed out and a band-pass filtering in the range 0.008-0.09 Hz was performed.

Then, the images were corrected by the anatomical CompCorr method [12] and the Functional Connectivity Toolbox (CONN) on a MATLAB R2010b platform. Finally, the images of each subject were divided into 90 ROIs by the automatic anatomical labeling [13] and from each ROI the time series were extracted removing the first 10 scans.

Figure 5: *BOLD signals used in this work*

180 columns = subjects initially considered; 90 rows = active areas (ROIs) considered for each subject under Resting State condition (closed eyes, no external stimulations, etc.).

Figure 6: *Thresholding and binarizing the BOLD signal*

(A) = the normalized BOLD signal (z-score values) is thresholded at 4 levelsin terms of Standard Deviation (0.25-0.50-0.75-1). The same criteria is applied to both positive and negative values;

(B): thresholded signals in which only values above the positive threshold and below the negative threshold are considered.

(C): coding of positive and negative activations by +1 and -1 values, respectively.

Figure 7: *Deriving Mutual Information values.*

a),b) = binarized activity time series (fragments) from signals of the type in Figure 3.

In (I) and (II) 1, 0, -1 correspond, respectively, to positive, null and negative activity peaks

c) Frequencies) of the 1, 0 -1 peaks type in the a) and b) fragments, indicated as independent probabilities (P).

d) Coupled frequencies/probabilities of the 1, 0, -1 peaks in the a and b fragments (Pab*) and the corresponding mutual information (Iab).